Journal of Applied Polymer Science

Determination of Moisture Content of Polyamide 66 Directly from Combination Region Near-Infrared Spectra

Chamathca P. S. Kuda-Malwathumullage, Gary W. Small
Department of Chemistry and Optical Science and Technology Center, University of Iowa, Iowa City, Iowa 52242
Correspondence to: G. W. Small (E-mail: gary-small@uiowa.edu)

ABSTRACT: The hygroscopic nature of polyamide (PA) polymers motivates the development of analysis tools for use in assessing their moisture content. Among possible analysis techniques, near-infrared (near-IR) spectroscopy is non-destructive, requires little or no sample preparation, and is compatible with sample thicknesses on the order of mm. The work reported here makes use of transmission near-IR spectroscopy in the combination region (5000–4000 cm^{-1}) to develop a protocol for assessing the moisture content of PA 66 samples directly from their spectral intensities after preprocessing with the standard normal variate transform and partial least-squares. The method is compatible with online or continuous monitoring applications and can be calibrated without the use of destructive reference measurements such as thermogravimetric analysis. The long-term calibration performance of the technique is evaluated, and on a scale of 0–100% moisture uptake, the standard error of prediction is found to average 1.4% over 6 months.
 J. Appl. Polym. Sci. **2014**, *131*, 40645.

KEYWORDS: optical properties; sensors and actuators; spectroscopy

Received 8 November 2013; accepted 27 February 2014
DOI: 10.1002/app.40645

INTRODUCTION

Polyamides (PAs) are a widely used class of polymers that have significant commercial importance.[1] These polymers have hygroscopic properties, meaning they absorb water from the surrounding environment.[2,3] Commercially available PA polymers can absorb up to an average of 8–10% of water by dry weight upon saturation.[4] The degree of affinity for water depends on the chemical structure of the PA species considered, and the rates of moisture uptake or subsequent moisture loss vary with the relative humidity, temperature, and the chemical structure of the specific PA considered.[4]

Moisture absorption of PA polymers has been a topic of interest for many years.[2,3,5] These polymers are sensitive to moisture due to their ability to form hydrogen bonds with water molecules using the polar amide groups.[2,6,7] This hydrogen bonding process is illustrated in Figure 1. Also, water molecules are believed to displace PA molecules, thereby resulting in swelling of the PA molecular matrix.[4] Water can act as a plasticizer which increases toughness and flexibility while reducing the tensile strength and modulus of PA polymers. Ultimately, absorption of moisture results in deterioration of electrical properties and poor dimensional stability in an environment of changing relative humidity.[7]

Most common techniques used in the determination of moisture content of a given PA are based on thermal analyses such as thermogravimetric analysis (TGA), differential scanning calorimetry (DSC), and loss-on-drying (LOD). Although these methods are reliable and easy to conduct, they are time-consuming and destructive. Hence, they cannot be used in online analyses.[2,3] Among chemical analysis methods, the Karl–Fischer titration is also used to determine the moisture content of PAs. Similar to the thermal analysis techniques, this method is also time-consuming, incompatible with online analyses and requires hazardous chemicals.[2]

Vibrational spectroscopy has also been used to characterize moisture content in PAs. This approach is attractive because it is nondestructive, requires little or no sample preparation and is potentially amenable to online analyses. Among the methods applied, both mid-infrared and near-infrared (near-IR) measurements have been performed. Mid-infrared approaches have the advantage of the use of fundamental vibrations, but strong absorption of light in this region from both water and the functional groups of the polymer limit these measurements to the analysis of thin films.[2,3]

By contrast, near-IR spectroscopy is compatible with polymer samples with considerable thickness (in the mm range) as the near-IR region exhibits reduced absorption when compared to the mid-infrared. The near-IR spectra of PAs have distinctive combination and overtone bands associated with C—H and N—H groups. However, the weak and highly overlapped spectral

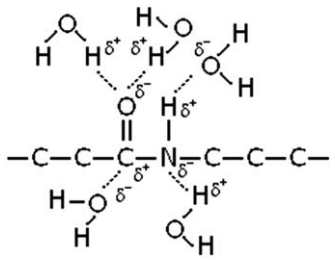

Figure 1. Schematic representation of moisture uptake on PA polymers. Water molecules form hydrogen bonds with polar amide groups in the PA structure.

features in the near-IR region present challenges when quantitative analyses are performed. Relating near-IR spectral intensities to quantitative measures such as moisture content requires the use of multivariate calibration techniques such as partial least-squares (PLS) regression.[8]

In previous work, Lachenal investigated the potential of near-IR spectroscopy to be used in the analysis of water content, degree of crystallinity, inter- and intra-molecular interactions of PAs, polyethylene terephthalate (PET), and polyurethane polymers.[3] Miller et al. used near-IR spectroscopy and chemometrics to analyze the morphology, amount of absorbed water, and the amount of adhesive present in polyethylene/PA laminates.[9] Both of these studies focused on studying the spectral features of specific polymers as they were subjected to changes in moisture content, temperature, etc. Neither investigated the ability to develop quantitative models to predict the moisture content of a given polymer.

Camacho et al. used near-IR spectroscopy and chemometrics to determine the moisture content of recycled PA 66 polymers using spectral features in the 4500–9000 cm^{-1} region.[2] This work was motivated by the premise that upon uptake of water, the overtones and combination peaks of PA 66 that arise due to the amide linkage are expected to deviate as a result of hydrogen bonding. Also, the intensities of the water bands themselves are expected to increase upon moisture uptake.

Camacho et al. documented the use of PLS regression to develop calibration models to predict moisture content in PA 66 polymers. In this study, however, the reference methods used for developing the calibration models were destructive methods such as TGA, DSC and LOD. This limits the integration of the method with routine nondestructive analysis procedures. Furthermore, the long-term predictive ability of the developed calibration models was not assessed.

Our laboratory has developed a number of quantitative methods in near-IR spectroscopy that focus specifically on the combination spectral region of 4000–5000 cm^{-1}.[10–14] This region lies between two intense and broad absorption bands of water that are centered near 3300 and 5200 cm^{-1},[15,16] and thus provides a spectral window in which samples, even those that contain a high water content, can be analyzed for a variety of chemical constituents[10,12,13] or physical properties.[14] Relative to other regions of the near-IR, spectral bands in the combination range are more intense, narrower, and have more defined shapes.[17] In addition, while diminished, significant water absorption remains and thus the water content of a sample can also be assessed. By optically isolating this region during the spectral acquisition, instrumental (e.g., source power on the detector) and experimental (e.g., optical path length) parameters can be optimized and therefore spectral quality can be maximized.

In the work discussed in this article, the methodology reported by Camacho is extended in several respects. Partial least-squares regression models are developed to determine the moisture content of PA 66 polymers directly from combination region near-IR spectra. The prediction performance of these moisture models is assessed for robustness with time and the ability to predict moisture uptake across different sheets of PA 66. The reliability of using an analytical balance as an alternative to time-consuming TGA measurements to obtain reference values for moisture content is also demonstrated in this work.

EXPERIMENTAL

Apparatus and Reagents

All spectral data collections were performed with a Bruker Vertex 70 (Bruker Optics, Billerica, MA) Fourier transform (FT) spectrometer configured with a tungsten-halogen lamp source, a calcium fluoride (CaF_2) beam splitter and a liquid nitrogen cooled indium antimonide (InSb) detector. A low-pass filter (OCLI, Santa Rosa, CA) was used to restrict the light beyond 5000 cm^{-1}. Commercially obtained PA 66 samples (McMaster-Carr, Elmhurst, IL) were used in this analysis. A metal sample holder was used to hold the samples. Weight measurements of the sample pieces were obtained with a Mettler AE200 analytical balance (Mettler-Toledo, Columbus, OH). A Fisher Scientific Isotemp Model 655G oven (Fisher Scientific, Pittsburgh, PA) and a glass desiccator equipped with drierite (W.A. Hammond Drierite, Xenia, OH) were used for drying purposes. Relative humidity measurements were obtained from a TES 1364 humidity-temperature meter (TES Electrical Electronic, Taipei, Taiwan). Thermogravimetric measurements made to establish reliable procedures for assessing moisture uptake were performed with a commercial TGA instrument (Model Q500-0305, TA Instruments, New Castle, DE).

Procedures

Near-Infrared Measurements. Six pieces of PA 66 (A, B, C, D, E, and F) were used in the spectral data collections. These samples were cut from three different commercially available sheets of PA 66 polymer. Samples A, B, C, D, E, and F were cut from PA 66 sheets 1, 2, 3, 1, 2, and 3, respectively. The average dimensions of the six samples were $25 \times 20 \times 0.40 \pm 0.01$ mm, and the average weight was 0.2350 ± 0.0001 g. All the spectral data collections were performed at ambient temperature conditions (~21–22°C). No efforts were made to control the sample temperatures.

Sample pieces were exposed to several methods of moisture uptake and drying. Methods of moisture uptake included soaking the PA in water, placing the PA piece in a humidity chamber and exposing the PA sample to ambient temperature and humidity conditions in the laboratory. Methods of drying

Table I. Summary of Spectral Collection Protocol for the Moisture Uptake Models

Data set	Number of samples[a]	Number of spectra collected	Time since calibration (weeks)
Calibration[b]	76	228	0
Prediction set 1 (PS01)	42	126	0.5
Prediction set 2 (PS02)	41	123	1
Prediction set 3 (PS03)	45	135	2
Prediction set 4 (PS04)	43	132	3
Prediction set 5 (PS05)	43	132	4
Prediction set 6 (PS06)	48	144	6
Prediction set 7 (PS07)	45	135	8
Prediction set 8 (PS08)	40	120	14
Prediction set 9 (PS09)	48	144	18
Prediction set 10 (PS10)	46	138	23

[a] A sample is defined as a piece of PA 66 subjected to a given level of moisture uptake.
[b] The calibration data used PA 66 pieces A and E while the prediction sets were recorded with pieces B, C, D, and F.

included drying in a desiccator, drying in an oven (~80 and ~100°C) and exposing the sample to ambient temperature and humidity conditions in the laboratory.

Moisture uptake was assessed by weighing the sample piece before and after exposure to water. The percentage moisture uptake of a given piece of PA 66, M, at a given time was calculated on the basis of the dry weight of the sample and is given in eq. (1).

$$M = \frac{W_{wet} - W_{dry}}{W_{dry}} \times 100 \quad (1)$$

In the equation, W_{wet} is the weight of a given piece of PA 66 with some absorbed moisture and W_{dry} is the weight of the sample at 0% moisture uptake.

A summary of the spectral collection protocol is given in Table I. For calibration purposes, spectra were collected from 76 PA 66 samples over three consecutive days using PA 66 pieces A and E. For this discussion, a sample is considered to be a specific piece of PA 66 subjected to a given set of moisture uptake conditions. Three consecutive spectra were collected from the sample after placing it in the spectrometer. A total of $3 \times 76 = 228$ calibration spectra were thus obtained. Each piece of PA 66 was weighed at the start and end of the spectral acquisition to allow the assessment of moisture loss during the 6 min of data acquisition time. This issue will be discussed in detail in a later section.

To assess the long-term predictive ability of the quantitative moisture models, 10 sets of spectra were collected using the other PA 66 pieces (B, C, D, and F) over a period of 6 months. Three replicate spectra were again collected for each sample.

Moisture uptake values were randomized in the calibration and prediction sets to minimize the correlation of moisture uptake with time. The method of moisture uptake and drying selected for a given piece of PA 66 was also randomized to assess the prediction performance of the moisture uptake model across different sheets of PA 66.

Open-beam air spectra were used as the background in the calculation of absorbance values throughout the data collection For a given data collection session, eight warm-up air spectra were collected at the beginning of the day and three intermediate air spectra were collected after the measurement of every fourth sample. An additional six air spectra were collected at the end of the day. The average of the air spectra collected on a given day was used in calculating the absorbance values for sample spectra collected on that day. A 6.3% metal thin-film neutral density filter (Rolyn Optics, Covina, CA) was used to attenuate the source intensity during the collection of the open-beam air spectra.

The raw data consisted of 256 coadded double-sided interferograms containing 14,220 points collected at every zero crossing of the helium-neon (He-Ne) reference laser. This corresponded to a maximum digitized frequency of 15,800.45 cm^{-1}. The nominal spectral resolution was 4 cm^{-1} and an aperture setting of 6 mm was used. All interferograms were Fourier processed to single-beam spectra by use of the Bruker Opus software controlling the spectrometer (Version 6.5, Bruker Optics). The single-beam spectra were computed with a point spacing of 1.9288 cm^{-1} by applying two levels of zero filling, Blackmann-Harris 3-Term apodization and Mertz phase correction. The wavenumber range selected for this study was from 4000 to 5000 cm^{-1}.

Further calculations were performed with Matlab (Version 7.4, The Mathworks, Natick, MA) on a Dell Precision 670 workstation (Dell Computer, Round Rock, TX) operating under Red Hat Linux WS (Version 5.2, Red Hat, Raleigh, NC). Nonlinear curve fitting to assess moisture loss with respect to time was performed with Microsoft Excel (Version 2007, Microsoft, Redmond, WA).

Before quantitative modeling of moisture uptake was investigated, the single-beam spectra of the PA 66 samples were converted to absorbance units by use of the appropriate open-beam air background. The resulting spectra were normalized by use of the standard normal variate (SNV) transform[18] applied over the

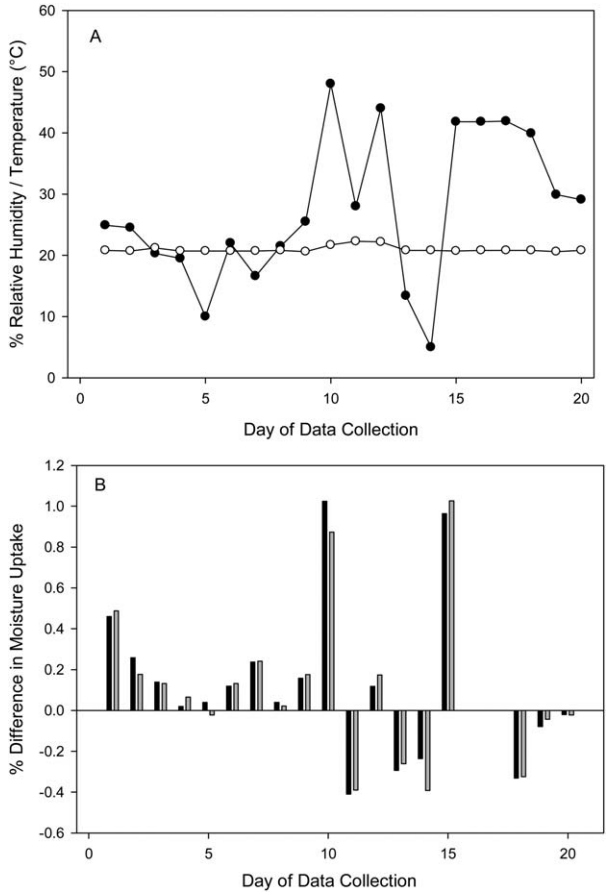

Figure 2. (A) Ambient % relative humidity (solid circles) and temperature measurements (open circles) obtained over the 20-day time period. (B) Moisture uptake pattern of PA 66 pieces B (black) and C (gray) over the 20-day time period. No data were taken on days 16 and 17.

4000–5000 cm^{-1} range. This method corrects for overall additive and multiplicative scaling effects by translating and scaling each spectrum to a mean of zero and a standard deviation of 1.0 absorbance units (AU).

Thermogravimetric Measurements. To assess the reliability of assigning moisture uptake values on the basis of measurements with the analytical balance, a set of parallel measurements was performed with TGA. Four pieces of PA 66 (average weight: 12.4 ± 0.1 mg) were dried in the oven to remove any moisture and subsequently weighed with the analytical balance. One piece each was taken from the original PA 66 sheets 1 and 2, while two pieces were taken from sheet 3. These were the same sheets of PA 66 from which the six pieces were taken for the near-IR measurements.

After weighing, the PA pieces were soaked in water until they were saturated. Weight measurements were then made on the saturated PA pieces before they were introduced to the TGA instrument. The temperature range analyzed in these experiments was from 20 to 600°C with a linear ramp of 5.00°C min^{-1}. The composition of the purge gas used was 19–23% O_2 in N_2. Once the PA sample was completely decomposed, the first derivative of the mass loss (peak centered at 100°C) with temperature was computed to calculate the % mass loss due to evaporation of water.

RESULTS AND DISCUSSION

Complementary Weight Measurements with TGA

Moisture uptake percentages obtained with the TGA method were well matched to the moisture uptake values commonly reported in commercial literature.[4] Also, moisture uptake percentages obtained with the TGA method were well correlated with the moisture uptake values obtained with the analytical balance. The percentage difference between the two methods ranged from −1.65% to +0.78%, with the mean absolute value of the percentage differences equal to 0.74%. A pairwise *t* test (two-tailed) to compare the two sets of % moisture uptake values was only significant at 47 % (mean and standard deviation of differences equal to −0.35% and 1.00%, respectively). These results suggest that the weight measurements obtained with the analytical balance were consistent with the TGA measurements and that the precision of the % moisture uptake values was on the order of ±1%. Based on these results, weight measurements obtained from the analytical balance were used subsequently in the development of calibration models for moisture uptake in PA.

Moisture Uptake of PA 66 and Relative Humidity

Two pieces of PA 66 (average weight: 0.2376 ± 0.0001 g) were dried in the oven to remove any moisture and weighed using the analytical balance. The two samples were then exposed to ambient relative humidity (RH) and temperature conditions in the laboratory for 20 days. Weight measurements were made on the samples each day using the analytical balance, and relative humidity and temperature measurements were performed with the humidity–temperature meter. As described by eq. (2), the moisture uptake pattern of the PA 66 pieces was expressed each day in relative terms compared to the previous day.

$$\Delta M = \frac{W_n - W_{n-1}}{W_n} \times 100 \quad (2)$$

In eq. (2), ΔM is the relative percentage change in moisture, W_n is the weight of the piece of PA 66 on day n, and W_{n-1} is the corresponding weight of the sample on the previous day

The trend in the moisture uptake pattern shown in Figure 2 clearly indicates the reversible nature of moisture uptake in PAs and its dependence on the relative humidity of the environment. For this experiment, the contribution of temperature was negligible as the laboratory temperature showed no significant change over the period of data collection.

Near Infrared Spectra of PA 66 Upon Water Uptake

Figure 3 illustrates near-IR absorbance spectra of PA 66 obtained at different levels of moisture uptake. The displayed spectra were normalized with the SNV transform. It can be observed that the intensity of absorption near 4000 and 5000 cm^{-1} is increasing with increasing moisture content. This is due to the presence of the two dominant water absorption peaks centered at 3300 cm^{-1} (fundamental O—H stretching) and 5200 cm^{-1} (combination band of O—H fundamental stretching and bending).

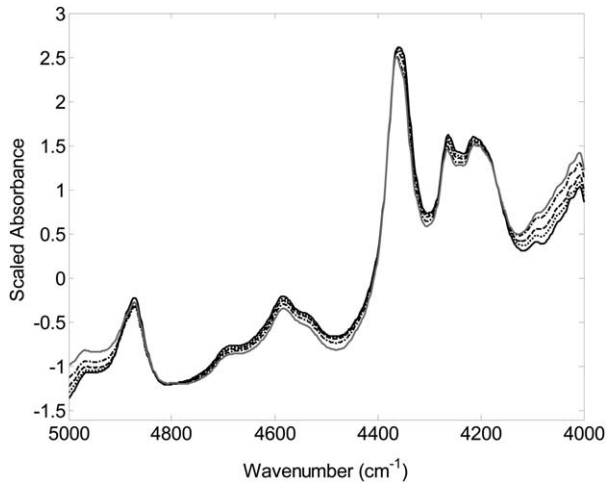

Figure 3. Near infrared spectra of PA 66 in the range of 4000–5000 cm^{-1} obtained at different levels of moisture uptake [eq. (1)]. Spectra were normalized with the SNV transform. Ordering of the spectra with respect to moisture uptake is observed at the two extremes of the plot as a consequence of the strong absorption bands of water near 3300 and 5200 cm^{-1}. Line types of solid black, dotted, dashed, dash-dot, and solid gray correspond to moisture uptake values of 0, 15, 35, 66, and 99%, respectively.

Application of a Correction Strategy for Moisture Loss During Spectral Acquisition

Possible moisture loss inside the spectrometer was of a concern as the relative humidity inside the sample compartment was measured to be 2–4%. Moisture loss during the spectral collection was investigated on the basis of assuming either a linear or an exponential decay. To test the two hypotheses, three pieces of PA 66 corresponding to initial values of 80, 65, and 45% moisture uptake [eq. (1)] were exposed to the dry conditions inside the sample compartment and weight measurements were obtained every 2 min for a total of 12 min. This time spacing corresponds to the collection of one replicate spectrum.

As described in eqs. (3–5), the moisture loss process was defined on the basis of Z, the % moisture remaining to be lost during the exposure to dry air. As a function of time, t, Z is defined as:

$$Z_t = \frac{\Delta W_{t-\max} - \Delta W_t}{\Delta W_{t-\max}} \times 100 \quad (3)$$

$$\Delta W_{t-\max} = W_{\text{initial}} - W_{t-\max} \quad (4)$$

$$\Delta W_t = W_{\text{initial}} - W_t \quad (5)$$

In eq. (3), $\Delta W_{t\text{-max}}$ corresponds to the total weight loss from time zero to the maximum time of the experiment (i.e., $t_{\max} = 12$ min (720 s) in the example described here). This is defined in eq. (4) as the difference between the initial weight, W_{initial}, and the weight after the maximum time, $W_{t\text{-max}}$. Experimentally, these initial and final weights are averages of three consecutive weight measurements taken at the beginning and end of the experiment, respectively. Similarly, ΔW_t corresponds to the weight loss at a given time, t, and is defined in eq. (5) as the difference between the initial weight, W_{initial}, and the weight at time, t, W_t.

Figure 4 plots the values of Z_t computed with $t_{\max} = 720$ s. These results suggest that moisture loss from the pieces of PA 66 follows an approximate exponential decay. If just the first 6 min are considered as the time required to collect three replicate spectra (i.e., $t_{\max} = 360$ s), about 49% of the total moisture loss (i.e., $Z_t = 51\%$ moisture remaining to be lost) occurred during the acquisition of the first replicate spectrum while about 36 and 15% of the total moisture loss occurred during the collection of the second and third replicate spectra, respectively.

On the basis of this experiment, an exponential decay correction was performed in order to assign a more accurate weight to the sample at the time of spectral collection. The data displayed in Figure 4 were fit to a simple exponential decay function, yielding the fitted result displayed in eq. (6) and represented as the solid line in Figure 4.

$$Z_t = 55.5e^{-0.00432t} + e_t \quad (6)$$

In the equation, e_t is the residual at time, t, that describes the error in the fit. This expression allows the value of Z_t to be estimated for any time (in seconds) within the range of 0 to the defined maximum time (e.g., 6 min in the context of acquiring three spectra). Given this estimated value along with the initial and final weights of the sample (i.e., W_{initial} and $W_{t\text{-max}}$, respectively), eqs. (3–5) can be combined and rearranged to solve for W_t:

$$W_t = \frac{Z_t}{100}(W_{\text{initial}} - W_{t-\max}) + W_{t-\max} \quad (7)$$

As an example, at $Z = 50\%$, eq. (7) simplifies to the weight at the time corresponding to the average of the initial and final weights.

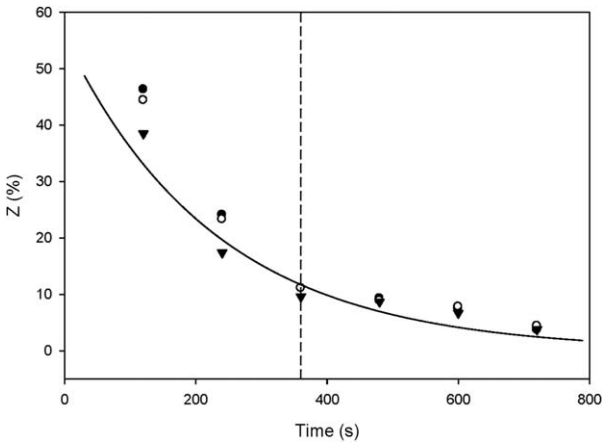

Figure 4. Values of Z_t [eq. (3)] obtained from three PA 66 pieces with respect to time of exposure to the dry atmosphere of the sample compartment of the spectrometer. The calculation of Z_t was based on $t_{\max} = 720$ s. The open circles, solid circles, and triangles correspond to 80, 65, and 45 initial values of % moisture uptake [eq. (1)], respectively. The solid line represents the results of fitting the data to an exponential decay function ($y = 55.5e^{-0.00432x}$). The value of r^2 corresponding to the fitted equation was 0.944. The last data points do not reach $Z_t = 0$ because $W_{t\text{-max}}$ [eq. (4)] is computed as the average of three replicate weights and is typically smaller than the single weight at the last time point due to further evaporation of water during the weighing procedure. The dashed line in the figure corresponds to the time required to collect three replicate spectra (360 s).

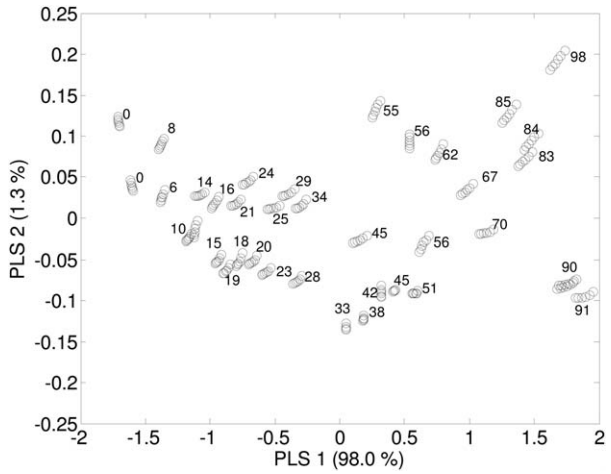

Figure 5. Partial least-squares score plot for factors 1 and 2 of PA 66 spectra used in the calibration model. Data labels are % moisture uptake values. More than 99% of the variance in the calibration data matrix is explained by the first two PLS latent variables. The values of % moisture uptake generally increase along a parabola that runs from the upper left to the upper right of the plot.

$$W_t = 0.5(W_{\text{initial}} - W_{t-\max}) + W_{t-\max} = 0.5W_{\text{initial}} + 0.5W_{t-\max} = \frac{W_{\text{initial}} + W_{t-\max}}{2} \quad (8)$$

Given the estimated weight at time t, eq. (1) can be used to estimate the corresponding % moisture uptake that corresponds to that time.

Assessment of the effectiveness of the exponential decay correction was performed by developing separate PLS calibration models for exponentially corrected and uncorrected % moisture uptake values. For the case of uncorrected values, the average weight of the sample before and after the spectral acquisition was assigned to each replicate spectrum.

In addition, a third model was built based on a simple linear decay function. For the linear function, the starting and ending weights and their corresponding times relative to the start of data acquisition (i.e., 0 and 6 min) were fit to a two-parameter linear model, and the resulting slope and intercept were used to assign a weight to each spectrum on the basis of its average collection time (i.e., 1, 3, and 5 min after the start of data collection).

The SNV-normalized absorbance spectra were used in computing the three models and both the wavenumber region submitted to the PLS procedure and the number of PLS model terms (latent variables) were optimized for each model by a grid-search procedure. This optimization protocol involved scanning the wavenumber range from 4000 to 5000 cm^{-1} in steps of 25 cm^{-1} using window sizes from 300 to 800 cm^{-1} in steps of 25 cm^{-1}. For each wavenumber range investigated, models based on 1–10 latent variables were computed. Cross-validation (CV) based on leaving out 10% of the calibration spectra per iteration was used to identify the optimal model. In this case, the CV procedure builds a model with 90% of the data and uses that model to predict the 10% withheld. By cycling through the withheld spectra, a cross-validated standard error of prediction (CV-SEP) can be computed to describe the model performance. The CV-SEP is an error estimate based on pooling the errors in predicted % moisture uptake for each of the spectra withheld from the calculation of the models. A smaller value of CV-SEP indicates better performance in prediction.

Once the spectral range associated with the minimum CV-SEP was determined, the optimal number of latent variables was taken as that which produced a value of CV-SEP not statistically different from the minimum CV-SEP. This determination was made by use of an F-test at the 95% confidence level.

For the exponentially corrected, linearly corrected, and uncorrected values of % moisture uptake, the CV-SEP values were 0.84, 1.13, and 1.93%, respectively. This suggests that the exponential decay correction addresses the moisture loss during the spectral collection effectively, thereby improving the predictive ability of the model. All further work reported here was performed with the exponentially corrected sample weights.

Evaluation of Spectral Noise

The quality and consistency of the spectra in the calibration and prediction sets was determined by the average root-mean-square (RMS) noise of spectra in each data set. This calculation was performed by taking the ratio of each pairwise combination of the three replicate single-beam spectra corresponding to a given moisture uptake level. The performance of the instrument itself was determined by the average RMS noise of air spectra for each day. This calculation was performed by taking the ratio of each pairwise combination of the replicate air spectra collected on a given day.

After taking the ratio, the resulting spectra were converted to absorbance units for the noise calculation. In this study, the spectral region from 4800 to 4200 cm^{-1} was used to compute the RMS noise. Systematic components in the noise spectra were removed by fitting the selected spectral region to a third-order polynomial function and computing the RMS noise in the resulting spectral residuals. Noise levels for both sample and air spectra were consistent across the time span of the data collection. Across the 11 data sets, the individual mean values of the noise levels for the air spectra in each data set ranged from 3.9 to 4.8 μAU, with an average of 4.3 μAU. The corresponding values for the PA 66 samples were a range of 59.1–73.7 μAU, and a mean value of 62.7 μAU. The noise levels observed for the PA spectra are higher, reflecting the reduction in transmitted light intensity caused by the presence of PA and water.

Calibration Models for Moisture Uptake on PA 66

To assess the ability to predict moisture uptake on PA 66 samples, PLS calibration models were generated from the SNV-normalized PA absorbance spectra in the calibration set and then applied to the 10 prediction sets. As described previously, a cross-validation procedure based on leaving out 10% of the calibration spectra per iteration was used to guide the optimization of the wavenumber range and number of latent variables. The best calibration model found was based on a wavenumber range of 4400–4000 cm^{-1} with three PLS factors. The CV-SEP value for this model was 0.65%.

Figure 5 is a score plot that illustrates the variance explained by the first two PLS factors computed from the optimized wavenumber range of the calibration spectra. The first PLS factor

Table II. Prediction Performance of PLS Calibration Models for Moisture Uptake on PA 66

Data set	SEP[a] (% moisture uptake)
Calibration[b]	0.84
PS01	1.32
PS02	1.17
PS03	1.28
PS04	0.96
PS05	1.40
PS06	1.23
PS07	1.57
PS08	1.06
PS09	1.93
PS10	1.74

[a] Moisture uptake percentages computed with eq. (1).
[b] Results reported for the calibration data are CV-SEP values.

explains 98% of the variance which is primarily the contribution from water itself. Together with the second PLS factor, a total of 99.3% of the data variance is explained. The points on the plot are labeled according to the corresponding values of

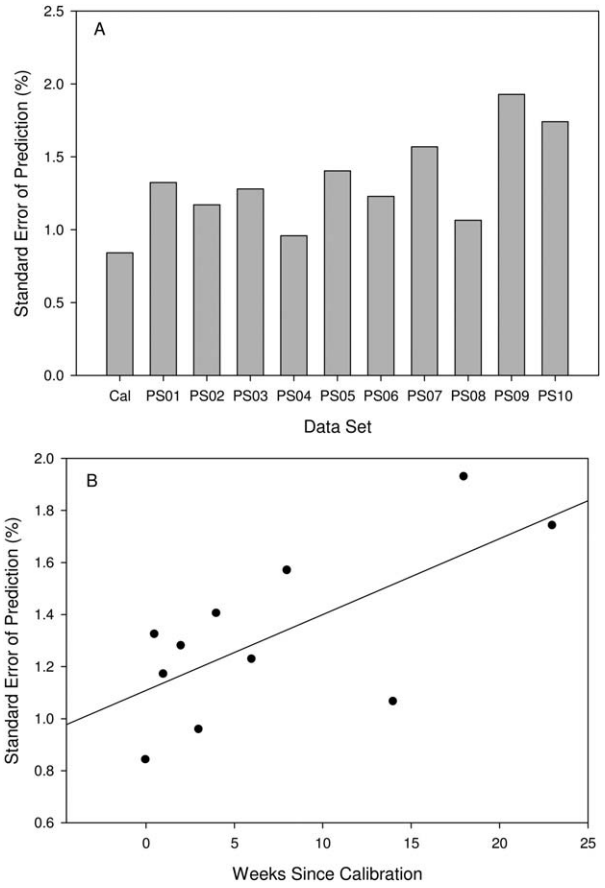

Figure 6. (A) Prediction performance of PLS calibration models for moisture uptake on PA 66. (B) Plot of SEP with respect to time since the calibration was performed. A slow degradation in performance (i.e., increase in SEP) can be seen across the ~6 months of data collection. A linear regression line is superimposed on the plot.

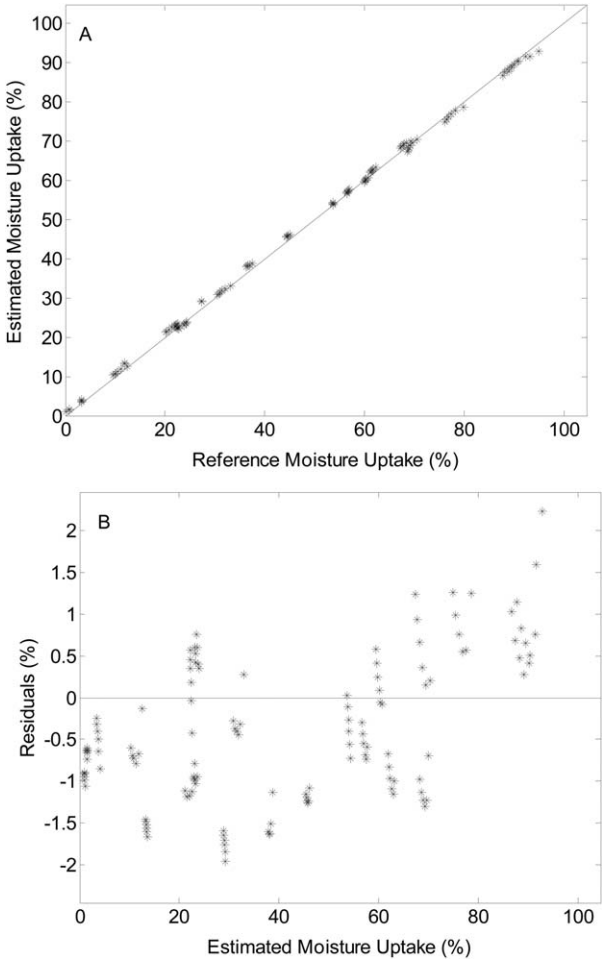

Figure 7. (A) Correlation and (B) residual plots for % moisture uptake in prediction set PS04. The solid lines in panels A and B correspond to perfect correlation between estimated and reference values of % moisture uptake and residuals of 0.0%, respectively.

% moisture uptake. In general, the values of % moisture uptake increase along a parabola that runs from the upper left to the upper right of the plot. Both PLS factors are clearly necessary to organize the data according to moisture content.

Prediction Performance of Moisture Uptake Models for PA 66

The long-term prediction performance of the moisture uptake models was assessed using the 10 prediction sets of PA 66 spectra collected over 6 months. The prediction performance of the models is summarized in Table II and Figure 6. The standard error of prediction (SEP) values reported in the table are a reflection of the standard deviation in the residuals (errors) between predicted and assigned (i.e., weight-based) values of % moisture uptake. These SEP values must be considered in the context of the 0 (dry) to 100% (saturated) range of the % moisture uptake values and the absolute error of roughly ±1% in the assigned values.

The calibration model gave good prediction results (SEP values ranging from 0.96 to 1.93%) which is indicative of the robustness of the models with time. These low SEP values also confirm the ability of the models to predict moisture uptake across

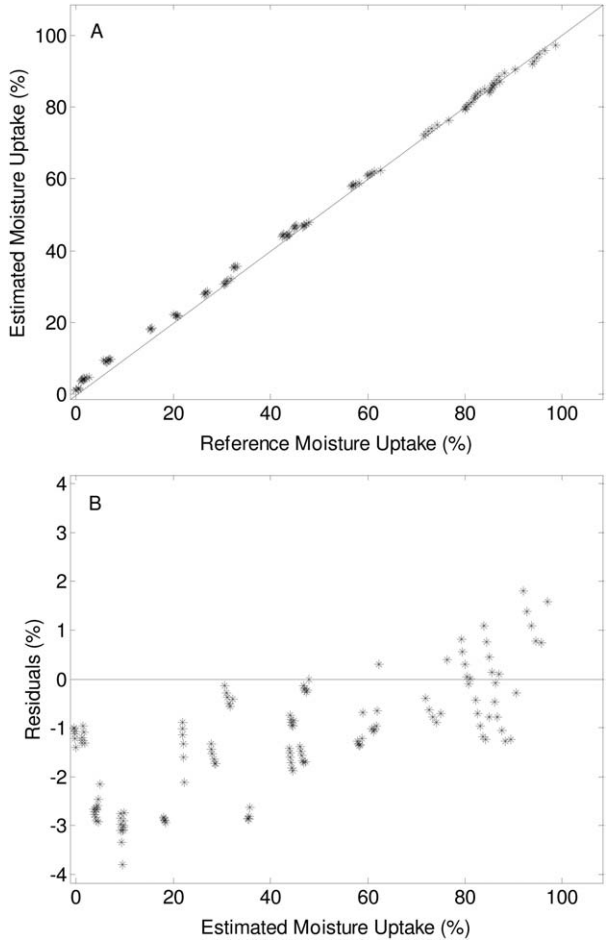

Figure 8. (A) Correlation and (B) residual plots for % moisture uptake in prediction set PS10. Some bias is evident in both plots. The solid lines in panels A and B correspond to perfect correlation between estimated and reference values and residuals of 0.0%, respectively.

different sheets of PA 66 polymers. Figure 6(B) plots the SEP values with respect to the time since the calibration data were recorded. While there is a gradual increase in SEP with time, we consider a 2% or smaller absolute error in % moisture uptake over 6 months to be a result good enough for practical use.

Figures 7 and 8 display correlation and residual plots for prediction sets PS04 and PS10, respectively. These data represent a time span of 3 and 23 weeks, respectively, relative to the collection of the calibration data. Overall, the prediction sets exhibit very good correlations between predicted and reference levels of % moisture uptake. However, as the time span increases relative to the calibration data, both correlation and residual plots exhibit some degradation in the model performance. This is particularly evident in the residual plots which begin to show some prediction bias.

CONCLUSIONS

Experimental results obtained in this study clearly indicate the reversible nature of moisture uptake of PAs and its dependence on the percentage RH of the environment. Experimental results also demonstrate that commercially available PA 66 polymers are capable of absorbing up to an average of 8–10% of water (relative to their dry weight) upon saturation. These findings motivate the need for practical measurement techniques to determine the moisture content of PA samples.

The quantitative analysis methodology developed in this work provides a practical way to measure the moisture content of PAs in a manner that is compatible with continuous monitoring or online applications. Furthermore, it was demonstrated that the method could be calibrated reliably with simple mass measurements, eliminating the need for destructive reference measurements such as TGA. The combination of spectral preprocessing by the SNV transform and PLS regression allowed the generation of successful calibration models directly from transmission near-IR spectra.

The long-term predictive performance of these moisture models was assessed using 10 prediction sets of PA 66 spectra at different moisture levels spanning a time period of 6 months. On a scale of 0–100% moisture uptake, the SEP values obtained for these prediction sets ranged from 0.96 to 1.93%, with an average $\pm$ standard deviation of 1.4% $\pm$ 0.3%. These models were also successful in predicting moisture uptake across different sheets of PA 66.

When compared to existing techniques (TGA, DSC, LOD, etc.), near-IR spectroscopy provides a reliable and fast method to determine the moisture content of a given PA polymer. This method can be applied to reasonably thick polymer sheets (e.g., in the mm range) as opposed to methods based on mid-infrared spectroscopy.

While beyond the scope of the present work, an interesting follow-on study would be to expand the calibration data to mimic more closely a specific industrial process or type of PA sample. For example, in a given application, the PA samples encountered may have surface contaminants that contribute their own signatures to the near-IR spectra. To handle such a case accurately, spectra with the appropriate signatures must be incorporated into the calibration data used to define the quantitative model.

Finally, the methodology developed in this work is not limited to PA 66, but could be applied to other PAs as well since all of the materials contain the amide linkage which is responsible for absorbing moisture. Furthermore, the methodology could be extended to other condensation polymers such as polyesters since they contain an ester linkage that follows a similar mechanism of moisture uptake as PAs.

REFERENCES

1. US Resin Production and Sales 2012 vs. 2011; American Chemistry Council: Washington, DC, **2013**. Available at: http://www.americanchemistry.com/Jobs/EconomicStatistics/Plastics-Statistics/Production-and-Sales-Data-by-Resin.pdf.
2. Camacho, W.; Valles-Liuch, A.; Ribes-Greus, A.; Karlsson, S. *J. Appl. Polym. Sci.* **2003**, *87*, 2165.
3. Lachenal, G. *Vib. Spectrosc.* **1995**, *9*, 93.
4. Nylon; San Diego Plastics, Inc. Available at: http://www.sdplastics.com/nylon.html, accessed on September **2013**.

5. Orendroff, C. J.; Huber, D. L.; Bunker, B. C. *J. Phys. Chem. C* **2009**, *113*, 13723.
6. Olabisi, O. Handbook of Thermoplastics; Marcel Dekker: New York, **1997**.
7. Ghosh, P. Polymer Science and Technology: Plastics, Rubbers, Blends and Composites; Tata McGraw-Hill: New Delhi, **2002**.
8. Small, G. W. *Trends Anal. Chem.* **2006**, *25*, 1057.
9. Miller, C. E.; Svendsen, S. A.; Næs, T. *Appl. Spectrosc.* **1993**, *47*, 346.
10. Ding, Q.; Boyd, B. L.; Small, G. W. *Appl. Spectrosc.* **2000**, *54*, 1047.
11. Kramer, K. E.; Small, G. W. *Appl. Spectrosc.* **2007**, *61*, 497.
12. Kramer, K. E.; Small, G. W. *Appl. Spectrosc.* **2009**, *63*, 246.
13. Sulub, Y.; Small, G. W. *Appl. Spectrosc.* **2007**, *61*, 406.
14. Kuda-Malwathumullage, C. P. S.; Small, G. W. *J. Appl. Polym. Sci.*, DOI: 10.1002/app.40476.
15. Libnau, F. O.; Kvalheim, O. M.; Christy, A. A.; Toft, J. *Vib. Spectrosc.* **1994**, *7*, 243.
16. Hazen, K. H.; Arnold, M. A.; Small, G. W. *Appl. Spectrosc.* **1994**, *48*, 477.
17. Chen, J.; Arnold, M. A.; Small, G. W. *Anal. Chem.* **2004**, *76*, 5405.
18. Luypaert, J.; Heuerding, S.; Vander Heyden, Y.; Massart, D. L. J. *Pharm. Biomed. Anal.* **2004**, *36*, 495.